

# Regularity and the Limit Cycle of the Van der Pol System: A Singular Perturbation Analysis

Emmanuel O. Ohwadia<sup>1</sup>, Stephen U. Egarievwe<sup>2</sup>

<sup>1</sup>Department of Mathematical Sciences, Bingham University, Karu, Nigeria

<sup>2</sup>Department of Industrial and Systems Engineering, Morgan State University, Baltimore, USA

Email: emmanuel.ohwadia@binghamuni.edu.ng

**How to cite this paper:** Ohwadia, E.O. and Egarievwe, S.U. (2026) Regularity and the Limit Cycle of the Van der Pol System: A Singular Perturbation Analysis. *Journal of Applied Mathematics and Physics*, **14**, 2317-2346.  
<https://doi.org/10.4236/jamp.2026.146114>

**Received:** May 6, 2026

**Accepted:** June 20, 2026

**Published:** June 23, 2026

Copyright © 2026 by author(s) and Scientific Research Publishing Inc. This work is licensed under the Creative Commons Attribution International License (CC BY 4.0).  
<http://creativecommons.org/licenses/by/4.0/>



Open Access

## Abstract

The Van der Pol oscillator, a definitive model for self-sustained nonlinear oscillations, exhibits a rich dynamical structure governed by the nonlinear damping parameter,  $\mu$ . While its limit cycle behaviour is well-established numerically, a comprehensive analytical characterization of the solution's regularity across the full spectrum of  $\mu$ , particularly in relation to the singular perturbation nature of the system, remains a subject of deep interest. This paper presents a unified singular perturbation analysis to rigorously examine the interplay between the regularity of solutions and the topological and geometric properties of the stable limit cycle. We decompose the problem into two asymptotic regimes. For the weakly nonlinear regime where the nonlinear damping parameter less than one but greater than zero, we employ the method of multiple scales to derive the asymptotic form of the limit cycle, proving its smooth dependence on the nonlinear damping parameter and establishing its amplitude and phase regularity. In the strongly nonlinear, relaxation oscillation regime where the nonlinear damping parameter is significantly greater than 1, we treat the system as a singularly perturbed dynamical system. Utilizing geometric singular perturbation theory and matched asymptotic expansions, we analysed the trajectory's structure—comprising slow drift along cubic critical manifolds and fast jumps. We explicitly characterize the loss of differentiability at the fold points (turning points) and demonstrate how this singularity is resolved in the composite solution, leading to a continuous but piecewise-smooth limit cycle in the infinite limit of  $\mu$ . Our central result bridges these regimes, providing a continuous description of how the limit cycle's regularity evolves from infinitely differentiable to piecewise differentiable as the nonlinear damping parameter tends to zero and infinity respectively. This work not only clarifies the intrinsic mathematical structure of the Van der Pol system but also provides a template for analysing regularity transitions in a broad class of singularly perturbed nonlinear oscillators.

## Keywords

Van der Pol Oscillator, Limit Cycle, Regularity, Singular Perturbation, Relaxation Oscillations, Matched Asymptotic, Geometric Singular Perturbation Theory

---

## 1. Introduction

The Van der Pol oscillator is a non-linear differential equation originally introduced by the Dutch physicist Balthasar van der Pol in 1920 [1] while he was studying vacuum tube circuits. He observed that these circuits could generate stable, periodic oscillations even without a periodic input signal—this inherent ability to oscillate is referred to as self-oscillation. Unlike the simple harmonic oscillator, which is linear and produces oscillations with a constant amplitude that depends on initial conditions, the Van der Pol oscillator is nonlinear. This nonlinearity of the equation is crucial because it allows the system to sustain oscillations of a stable amplitude, regardless of the initial conditions (as long as they are not trivial, *i.e.*, at the equilibrium point). The equation models a non-conservative system in which energy is added to and subtracted from the system, resulting in a stable amplitude known as a limit cycle [2]. Unlike a simple pendulum (approximated as a harmonic oscillator) which will eventually stop due to damping—to keep it swinging, you need to push it periodically. However, the Van der Pol oscillator has a built-in mechanism that provides energy when oscillations are small and dissipates energy when oscillations are large, thus regulating its own amplitude [3].

It is observed that while the limit cycle's existence is known, a detailed analytical study of the regularity (smoothness) of its solutions as a function of  $\mu$ —particularly through the lens of singular perturbation theory is lacking—emphasizing the singular nature of the  $\mu \rightarrow \infty$  limit. Mathematically, a singularity is a point, at which a function is not defined (discontinuous) or behaves erratically or blows up [4], for instance  $f(x) = 1/x$ , at  $x = 0$ . On the other hand, regularity of differential equations refers to the smoothness and well-behaved nature of their solutions, which depends fundamentally on the properties of the equations themselves. A differential equation is considered regular when it possesses solutions that are sufficiently smooth (differentiable and integrable) and can be characterized by standard mathematical techniques, meaning the coefficients and forcing terms are well-defined and continuous over the domain of interest [5]. Understanding regularity is thus essential for selecting appropriate analytical and numerical methods, predicting solution behaviour, and establishing the mathematical foundations for modelling physical phenomena.

In ordinary differential equations, regularity is closely tied to existence and uniqueness theorems. The Picard-Lindelöf theorem, for instance, guarantees that if the right-hand side of a first-order ODE is Lipschitz continuous, then a unique

solution exists locally [6]. Higher regularity of solutions, such as continuous differentiability to various orders, typically requires correspondingly smooth coefficients in the equation. Linear differential equations with continuous coefficients generally produce regular solutions, while equations with discontinuous coefficients or singularities may exhibit irregular behaviour. While in the context of partial differential equations, regularity theory becomes more sophisticated and is central to understanding solution behaviour. Elliptic equations like Laplace's equation often produce very smooth solutions in the interior of domains, even when boundary data is less regular [7]. Parabolic equations such as the heat equation have smoothing properties that improve regularity over time [8]. Hyperbolic equations, like the wave equation, preserve regularity but don't generally improve it, and solutions may develop discontinuities or shocks even from smooth initial data, particularly in nonlinear cases [9].

Singular points represent locations where regularity breaks down. For ODEs, these are points where coefficients become infinite or undefined, leading to solutions that may grow unbounded or exhibit other irregular behaviours. The classification of singular points as regular or irregular singular points determines whether series solution methods can be applied effectively [5]. Regular singular points allow for generalized power series solutions using the Frobenius method, while irregular singular points require more sophisticated asymptotic techniques [10]. Understanding regularity is thus essential for selecting appropriate analytical and numerical methods, predicting solution behaviours, and establishing the mathematical foundations for modelling physical phenomena.

This study provides a continuous description of how the limit cycle's regularity evolves from infinitely differentiable ( $C^\infty$ ) for  $\mu \rightarrow 0$  to piecewise differentiable for  $\mu \rightarrow \infty$ . The work not only clarifies the intrinsic mathematical structure of the Van der Pol system but also provides a template for analysing regularity transitions in a broad class of singularly perturbed nonlinear oscillators. So, our goal is to provide a unified singular perturbation framework to characterize the transition in the limit cycle's regularity from the weakly nonlinear to the relaxation oscillation regime. The Van der Pol oscillator has since found applications across disciplines, including biology, neuroscience, and mechanical engineering and in various fields like physics and engineering to model systems with damping that depends on the amplitude.

In the remaining part of this paper, we shall discuss the Van der Pol oscillator by unveiling the governing equation, its characteristics and via limit cycle perturbation, followed by Section 2 with discussion on the Van der Pol equation, and Section 3 focuses on the numerical solution using the Radau IIA method with its implementation. Section 4 deals with the singularity and regularity theory of the Van der Pol equation, while Sections 5 and 6 presents the discussions on findings, and conclusions and recommendations.

## 2. The Van der Pol Equation

The governing equation for the Van der Pol oscillator is a second-order nonlinear

ordinary differential equation:

$$\ddot{x} - \mu(1-x^2)\dot{x} + x = 0, \quad \mu > 0 \quad (1)$$

where

- $x$  is the position and represents the displacement or some other system variable (e.g., voltage in an electrical circuit).
- $t$  is time.
- $\mu$  is a positive parameter that controls the strength of the nonlinearity and the damping.

The scalar parameter  $\mu$  indicates the nonlinearity and the strength of the damping. When  $\mu = 0$ , it should reduce to the simple harmonic oscillator, which is linear. But when  $\mu > 0$ , the system becomes nonlinear with damping that is negative for small amplitudes (leading to growth) and positive for large amplitudes (leading to dissipation), resulting the limit cycle behaviour.

### 2.1. Characteristics of Van der Pol Oscillator

**First Restoring Force Term (+x):** This is analogous to the spring force in a simple harmonic oscillator. It pulls the system back towards the equilibrium point ( $x = 0$ ). If this were the only term along with the acceleration, there would be a simple harmonic motion.

**Damping/Driving Term ( $-\mu(1-x^2)\dot{x}$ ):** This is the heart of the nonlinearity and what makes the Van der Pol oscillator self-oscillating. The term  $\dot{x}$  represents the velocity. The term  $(1-x^2)$  is the key. The behaviour of  $x$  can further be interpreted as follows:

- When  $|x| < 1$  (near the equilibrium): The term  $(1-x^2)$  is positive. Therefore,  $-\mu(1-x^2)\dot{x}$  acts as negative damping or a driving force. This means that when the oscillation is small, the system gains energy, causing the amplitude to grow.
- When  $|x| > 1$  (far from the equilibrium): The term  $(1-x^2)$  is negative. Therefore,  $-\mu(1-x^2)\dot{x}$  acts as positive damping or a dissipating force. This means that when the oscillation is large, the system loses energy, causing the amplitude to shrink.
- At instants when  $|x| = 1$  the damping force momentarily vanishes [11].

This ingenious damping term ensures that if the oscillation starts small, it grows until  $x$  is large enough for the damping to become positive and limit the growth. Conversely, if the oscillation starts large, it shrinks until  $x$  is small enough for the damping to become negative and prevent further decay. This dynamic balance leads to a stable limit cycle.

### 2.2. Derivation of the Van der Pol Equation via Limit Cycle Perturbation

The limit cycle perturbation (or amplitude-dependent damping) method provides a framework for deriving the Van der Pol equation by analysing how damping

depends on oscillation amplitude. The method assumes a weakly nonlinear oscillator where damping and restoring forces are perturbed, leading to the characteristic limit cycle behaviour where small amplitudes are amplified, and large amplitudes are damped [12] [13]. The derivation starts from a simple harmonic oscillator and introduces a small, amplitude-dependent damping term whose sign changes with amplitude, leading to a stable limit cycle. The resulting equation is shown to be exactly the Van der Pol equation after appropriate scaling.

Setup

Consider an undamped linear harmonic oscillator:

$$\ddot{x} + x = 0 \quad (2)$$

with total mechanical energy,

$$E = \frac{1}{2}(\dot{x}^2 + x^2) \quad (3)$$

For the linear oscillator,  $E$  is constant. The time derivative of the energy is identically zero:

$$\frac{dE}{dt} = \dot{x}\ddot{x} + x\dot{x} = \dot{x}(-x) + x\dot{x} = 0 \quad (4)$$

Now suppose we introduce a small, nonlinear damping term  $\varepsilon f(x, \dot{x})$  to the right-hand side of (2), we have,

$$\ddot{x} + x = \varepsilon f(x, \dot{x}) \quad (5)$$

where  $0 < \varepsilon \ll 1$ . The energy evolution becomes:

$$\frac{dE}{dt} = \dot{x}\ddot{x} + x\dot{x} = \dot{x}(-x + \varepsilon f(x, \dot{x})) + x\dot{x} = \varepsilon \dot{x}f(x, \dot{x}) \quad (6)$$

Now, for the oscillator to exhibit a stable limit cycle (isolated periodic orbit), the net energy gain over one period must be zero, with small-amplitude oscillations gaining energy and large-amplitude oscillations losing energy.

Choice of Damping Function

We seek a function  $f(x, \dot{x})$  such that:

- For small amplitude ( $|x| \ll 1$ ,  $|\dot{x}| \ll 1$ ), we have  $\frac{dE}{dt} > 0$  (energy input, negative damping).
- For large amplitude,  $\frac{dE}{dt} < 0$  (energy dissipation, positive damping).
- The function should be odd in  $\dot{x}$  (to preserve symmetry between expansion and contraction), and simplest to lowest order.

The simplest polynomial satisfying these conditions can be given as:

$$f(x, \dot{x}) = (1 - x^2)\dot{x} \quad (7)$$

For small  $x$ :  $f \approx \dot{x}$ , giving  $\frac{dE}{dt} \approx \varepsilon \dot{x}^2 > 0$ .

While for large  $x$ :  $f \approx -x^2\dot{x}$ , giving  $\frac{dE}{dt} \approx -\varepsilon x^2\dot{x}^2 < 0$ .

The transition is expected to occur around  $|x| \approx 1$ .

Thus, Equation (6) becomes:

$$\ddot{x} + x = \varepsilon(1 - x^2)\dot{x} \quad (8)$$

Non-dimensionalization and Parameter Scaling

Equation (8) already contains a small parameter  $\varepsilon$ . However, the classical Van der Pol equation is usually written with a single parameter  $\mu > 0$  not necessarily small:

$$\ddot{x} + x = \mu(1 - x^2)\dot{x} \quad (9)$$

If  $\mu$  is small, Equation (9) is a weakly nonlinear oscillator. The scaling  $\varepsilon \equiv \mu$  recovers Equation (8). No further non-dimensionalization is needed; where Equation (8) is the Van der Pol equation in standard form. If we wish to make the nonlinear term  $O(1)$  while retaining a perturbation parameter, we can rescale time such that  $t = \tau/\sqrt{\mu}$ . However, for relaxation oscillations ( $\mu \gg 1$ ), one rescales differently. But for the derivation from limit cycle perturbation, we keep  $\varepsilon$  small. Hence:

$$\ddot{x} - \varepsilon(1 - x^2)\dot{x} + x = 0 \quad (10)$$

with  $\varepsilon > 0$  small. This is exactly the Van der Pol equation.

Our derived Equation (10) has  $\varepsilon$  instead of  $\mu$ . If we set  $\mu = \varepsilon$ , the two are identical, and we can write the Van der Pol equation as:

$$\ddot{x} - \mu(1 - x^2)\dot{x} + x = 0 \quad (11)$$

### 3. Numerical Solution of the Van der Pol Equation Using Radau IIA Method

The Van der Pol oscillator generally lacks analytical or exact solutions, particularly for non-zero values of  $\mu$ . Therefore, a numerical approach is necessary. Radau IIA methods, is the adaptive order Radau method in Fortran due to Hairer, and they are known to be state-of-the-art for the high-accuracy solution of highly stiff ordinary differential equations (ODEs) [14]. Radau methods are defined by quadrature formulas with higher order accuracy and strong stability properties which are crucial to ensure that the numerical method can handle the perturbations. Radau IIA is an implicit Runge-Kutta method of order  $2s-1$  for an  $s$ -stage scheme. The most common implementation uses  $s = 3$  stages, giving 5th order accuracy. Below is a comprehensive explanation of the Radau IIA algorithm as applied to the Van der Pol equation. This includes the mathematical formulation, the step-by-step computational process, and a simplified implementation to illustrate the inner workings.

#### 3.1. Mathematical Formulation

##### Problem Restatement

The Van der Pol equation of (1) above is converted to a first-order system:

$$\begin{cases} \frac{dx}{dt} = f_1(t, x, y) = y \\ \frac{dy}{dt} = f_2(t, x, y) = \mu(1-x^2)y - x \end{cases} \quad (12)$$

Let

$$\mathbf{u} = \begin{bmatrix} x \\ y \end{bmatrix} \quad \text{and} \quad \mathbf{f}(t, \mathbf{u}) = \begin{bmatrix} y \\ \mu(1-x^2)y - x \end{bmatrix} \quad (13)$$

Then:

$$\frac{d\mathbf{u}}{dt} = \mathbf{f}(t, \mathbf{u}), \mathbf{u}(t_0) = \mathbf{u}_0 \quad (14)$$

The general  $s$ -stage implicit Runge-Kutta method is:

$$\mathbf{u}_{n+1} = \mathbf{u}_n + \Delta t \sum_{i=1}^s b_i \mathbf{k}_i \quad (15)$$

where the stage derivatives  $\mathbf{k}_i$  are defined implicitly:

$$\mathbf{k}_i = \mathbf{f} \left( t_n + c_i \Delta t, \mathbf{u}_n + \Delta t \sum_{j=1}^s a_{ij} \mathbf{k}_j \right), i = 1, \dots, s \quad (16)$$

where:

- $c_i$  are the stage time points (abscissae).
- $a_{ij}$  are the Runge-Kutta coefficients.
- $b_i$  are the weights.

#### Algorithm for One Time Step

Given:

- Current solution  $\mathbf{u}_n$  at time  $t_n$ .
- Time step  $\Delta t$ .
- Function  $\mathbf{f}(t, \mathbf{u})$ .

**Step I:** Set up the nonlinear system for  $\mathbf{k}_1, \mathbf{k}_2, \mathbf{k}_3$ :

For  $i = 1, 2, 3$ :

$$\mathbf{k}_i = \mathbf{f} \left( t_n + c_i \Delta t, \mathbf{u}_n + \Delta t \sum_{j=1}^3 a_{ij} \mathbf{k}_j \right) \quad (17)$$

This is a system of  $3 \times 2 = 6$  equations (since  $\mathbf{k}_i$  are 2D vectors). Let  $\mathbf{K}$  be the vector of all stages such that,

$$\mathbf{K} = \begin{bmatrix} \mathbf{k}_1 \\ \mathbf{k}_2 \\ \mathbf{k}_3 \end{bmatrix} \in \mathbb{R}^6 \quad (18)$$

Let us define the residual function as:

$$\mathbf{R}(\mathbf{K}) = \mathbf{K} - \mathbf{F}(\mathbf{K}) = 0 \quad (19)$$

where  $\mathbf{F}(\mathbf{K})$  contains the right-hand side evaluations.

**Step II:** Solve the nonlinear system using Newton's method:

**Newton iteration:**

$$\mathbf{K}^{(m+1)} = \mathbf{K}^{(m)} - \left[ \mathbf{I} - \frac{\partial \mathbf{F}}{\partial \mathbf{K}}(\mathbf{K}^{(m)}) \right]^{-1} \mathbf{R}(\mathbf{K}^{(m)}) \tag{20}$$

where  $\frac{\partial \mathbf{F}}{\partial \mathbf{K}}$  is the  $6 \times 6$  Jacobian matrix of the stage equations.

**Step III:** Once converged to tolerance, we compute the new solution thus,

$$\mathbf{u}_{n+1} = \mathbf{u}_n + \Delta t \sum_{i=1}^3 b_i \mathbf{k}_i \tag{21}$$

However, due to stiff accuracy, we have,

$$\sum_j a_{3j} = b_j \text{ and } c_3 = 1 \tag{22}$$

we also have,

$$\mathbf{u}_{n+1} = \mathbf{u}_n + \Delta t \mathbf{k}_3 \tag{23}$$

### 3.2. Detailed Newton Iteration for Van der Pol

**Step I:** Define the Stage Inputs

For each stage  $i = 1, 2, 3$ :

$$\mathbf{U}_i = \mathbf{u}_n + \Delta t \sum_{j=1}^3 a_{ij} \mathbf{k}_j \text{ and } T_i = t_n + c_i \Delta t \tag{24}$$

Let  $\mathbf{k}_i = \begin{bmatrix} k_{i,x} \\ k_{i,y} \end{bmatrix}$ ,

**Step II:** Stage Equations

$$\mathbf{R}_i(\mathbf{K}) = \mathbf{k}_i - \mathbf{f}(T_i, \mathbf{U}_i) = 0 \tag{25}$$

For the Van der Pol system, we have,

$$\begin{aligned} f_x(t, \mathbf{u}) &= y \\ f_y(t, \mathbf{u}) &= \mu(1 - x^2)y - x \end{aligned} \tag{26}$$

Thus,

$$\mathbf{R}_i = \begin{bmatrix} k_{i,x} - U_{i,y} \\ k_{i,y} - [\mu(1 - U_{i,x}^2)U_{i,y} - U_{i,x}] \end{bmatrix} = 0 \tag{27}$$

**Step III:** Jacobian Matrix  $\frac{\partial \mathbf{F}}{\partial \mathbf{K}}$

The Jacobian has a block structure. For stage  $i$  and stage  $j$ , we have,

$$\frac{\partial \mathbf{F}_i}{\partial \mathbf{k}_j} = \frac{\partial \mathbf{f}}{\partial \mathbf{u}}(T_i, \mathbf{U}_i) \cdot (\Delta t a_{ij} \mathbf{I}_2) \tag{28}$$

where,

$$\mathbf{J}_f = \frac{\partial \mathbf{f}}{\partial \mathbf{u}} = \begin{bmatrix} 0 & 1 \\ -2\mu xy - 1 & \mu(1 - x^2) \end{bmatrix} \tag{29}$$

So,

$$\frac{\partial \mathbf{F}_i}{\partial \mathbf{k}_j} = \Delta t a_{ij} \mathbf{J}_f(T_i, \mathbf{U}_i) \tag{30}$$

and the full  $6 \times 6$  Jacobian becomes,

$$\frac{\partial \mathbf{F}}{\partial \mathbf{K}} = \Delta t \begin{bmatrix} a_{11} \mathbf{J}_1 & a_{12} \mathbf{J}_1 & a_{13} \mathbf{J}_1 \\ a_{21} \mathbf{J}_2 & a_{22} \mathbf{J}_2 & a_{23} \mathbf{J}_2 \\ a_{31} \mathbf{J}_3 & a_{32} \mathbf{J}_3 & a_{33} \mathbf{J}_3 \end{bmatrix} \quad (31)$$

where  $\mathbf{J}_i = \mathbf{J}_f(T_i, \mathbf{U}_i)$ .

The Newton matrix appears as,

$$\mathbf{M} = \mathbf{I}_6 - \frac{\partial \mathbf{F}}{\partial \mathbf{K}} \quad (32)$$

**Step IV:** Newton Update

We then solve the linear system given as,

$$\mathbf{M} \Delta \mathbf{K} = -\mathbf{R}(\mathbf{K}^{(m)}) \quad (33)$$

with,

$$\mathbf{K}^{(m+1)} = \mathbf{K}^{(m)} + \Delta \mathbf{K} \quad (34)$$

### 3.3. Implementation Using Python

The numerical solution of the Van der Pol oscillator using the Radau IIA method, is implemented with Python programming language. The initial condition is  $x(0) = a$ ,  $\dot{x}(0) = b$ , produce:

- time-domain plots  $(x, t)$ ,
- velocity-time plots  $(\dot{x}, t)$ ,
- acceleration-time plots  $(\ddot{x}, t)$ ,
- Phase portraits (limit cycle).

**Parameters:**

- Mu ( $\mu$ ): Nonlinearity parameter ( $\mu > 0$  creates self-sustaining oscillations),
- $a, b$ : Initial conditions for position and velocity,
- $t_0, t_f$ : Simulation time range,
- $h$ : Step size for numerical integration.

#### Interpretations

**Figure 1 ( $\mu = 0.1$ ):**

**Figure 1** illustrates the behaviour of the weakly nonlinear Van der Pol oscillator when the nonlinearity parameter is small ( $\mu = 0.1$ ). In this regime, the system behaves almost like a classical harmonic oscillator, but with a slight nonlinear damping effect. The time-history plots of displacement  $x(t)$  and velocity  $y(t)$  show nearly sinusoidal oscillations with smooth periodic motion. Because the nonlinear damping is weak ( $\mu \ll 1$ ), the oscillator gradually adjusts its amplitude until it reaches a stable periodic orbit. The numerical solution gives a steady-state amplitude of approximately 1.97, which is very close to the theoretical limit-cycle amplitude of 2. This confirms the existence of a stable self-sustained oscillation predicted by the singular perturbation analysis. The phase portrait ( $y$  versus  $x$ ) forms a smooth closed curve surrounding the origin. This closed trajectory represents the stable limit cycle of the system. Since trajectories neither spiral outward

indefinitely nor decay to zero, the figure demonstrates that the nonlinear damping mechanism injects energy into small oscillations while dissipating energy from large oscillations until a balanced periodic state is reached. The oscillation period remains relatively short and regular, indicating that the system is only mildly nonlinear. Hence, **Figure 1** confirms the transition from linear harmonic behaviour to weak nonlinear self-excited oscillation.

**Figure 2 ( $\mu = 0$ ):**

**Figure 2** represents the special case where the nonlinearity parameter vanishes ( $\mu = 0$ ). The governing equation therefore reduces to the simple harmonic oscillator equation:  $\ddot{x} + x = 0$ , which contains no nonlinear damping term. The displacement and velocity plots show purely sinusoidal oscillations with constant amplitude throughout the simulation interval. Unlike the nonlinear cases, there is no mechanism for amplitude growth or decay. Consequently, the oscillator conserves energy and exhibits neutral stability. The phase portrait is an ellipse (or nearly circular closed orbit depending on scaling), which is characteristic of a conservative linear oscillator. Every trajectory corresponds to a constant-energy orbit rather than an isolated attracting limit cycle. Thus, the orbit is not asymptotically stable because neighbouring trajectories do not converge toward a unique periodic solution. The results therefore demonstrate that the nonlinear damping term in the Van der Pol system is solely responsible for the emergence of the stable limit cycle. **Figure 2** serves as the linear reference case against which the nonlinear oscillatory behaviour is compared.

**Figure 3 ( $\mu = 5.0$ ):**

**Figure 3** shows the behaviour of the Van der Pol system for a moderate nonlinear parameter ( $\mu = 5$ ), where strong nonlinear effects begin to dominate the dynamics. The displacement-time graph reveals oscillations that are no longer sinusoidal. Instead, the solution exhibits slow variations followed by rapid transitions, indicating the onset of relaxation oscillations. These rapid jumps occur because the nonlinear damping strongly separates the motion into slow and fast dynamical phases. The velocity profile displays sharp spikes, with the numerical solution showing significantly larger velocity magnitudes compared with the weakly nonlinear case. The acceleration values also become very large, reflecting the sudden fast transitions between branches of the motion. The phase portrait develops into a strongly distorted closed curve with sharp corners and elongated segments. This geometric deformation is characteristic of relaxation oscillations in singular perturbation theory. The trajectory still converges to a stable limit cycle, but the cycle is now highly nonlinear and non-sinusoidal. The oscillation period increases substantially compared with **Figure 1**, indicating that the system spends a long time evolving slowly before undergoing rapid transitions. This slow-fast structure is a hallmark of singularly perturbed systems and confirms the theoretical predictions of the Van der Pol relaxation mechanism. Hence, **Figure 3** demonstrates the transition from weakly nonlinear oscillation to pronounced relaxation oscillation behaviour.

**Figure 4 ( $\mu = 10.0$ ):**

**Figure 4** illustrates the strongly nonlinear regime of the Van der Pol oscillator for a large parameter value ( $\mu = 10$ ). In this case, the singular perturbation structure becomes dominant. The time-series plots clearly show classical relaxation oscillations. The displacement evolves slowly over long intervals and then changes abruptly during extremely rapid transitions. These sudden jumps correspond to fast dynamics occurring near the turning points of the slow manifold. The velocity and acceleration attain very large magnitudes, demonstrating the stiffness of the differential equation. This validates the use of the implicit Radau IIA numerical method, which is particularly suitable for stiff systems. The phase portrait becomes nearly rectangular with steep vertical transitions and slow horizontal motion. This shape is typical of strongly nonlinear Van der Pol limit cycles and reflects the coexistence of slow and fast time scales predicted by singular perturbation analysis. The computed steady-state amplitude approaches the theoretical value of 2 with extremely small error, confirming the asymptotic prediction for large  $\mu$ . In addition, the oscillation period increases further, showing that the slow phases dominate the motion as the nonlinearity grows stronger. Overall, **Figure 4** confirms that for large  $\mu$ , the Van der Pol system evolves into a stiff relaxation oscillator possessing a unique, strongly attracting limit cycle. The figure provides strong numerical evidence for the regularity and asymptotic limit-cycle structure established in the research paper.

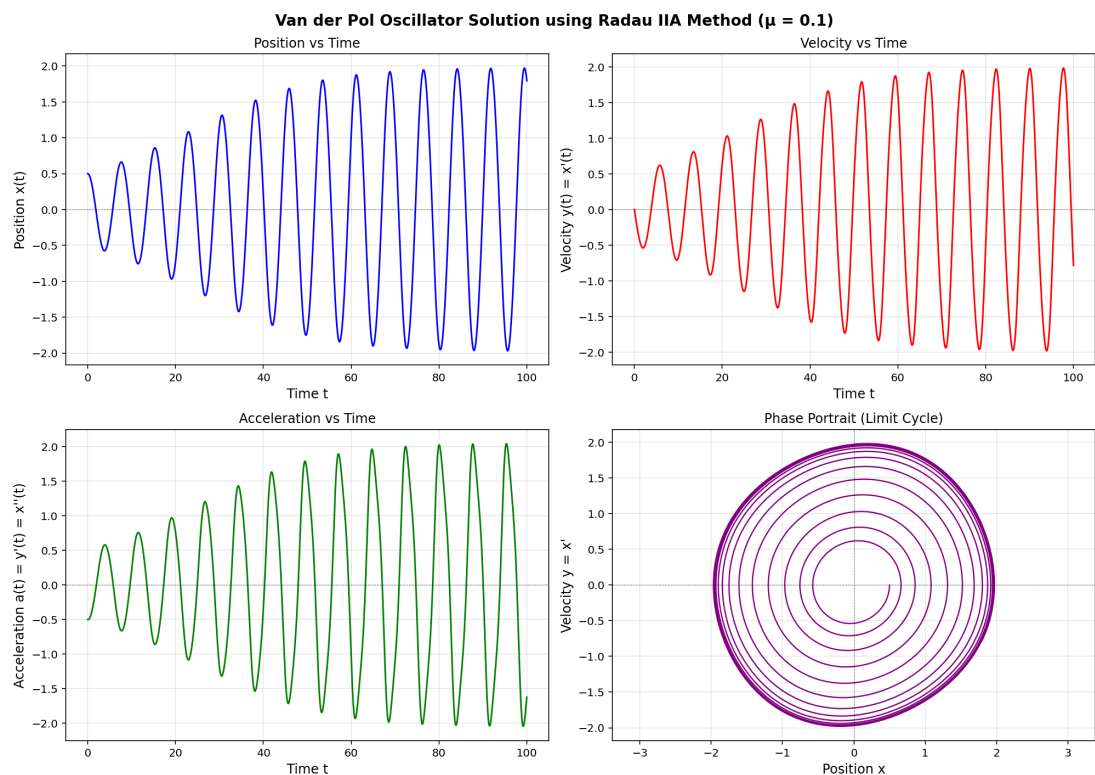


**Figure 1.** Typical solution of van der Pol equation (time versus displacement,  $x$  and velocity,  $\dot{x}$ ) and (velocity,  $\dot{x}$  versus displacement,  $x$ ) with initial  $x = 0.5$ ,  $\mu = 0.1$ ,  $h = 0.01$ .

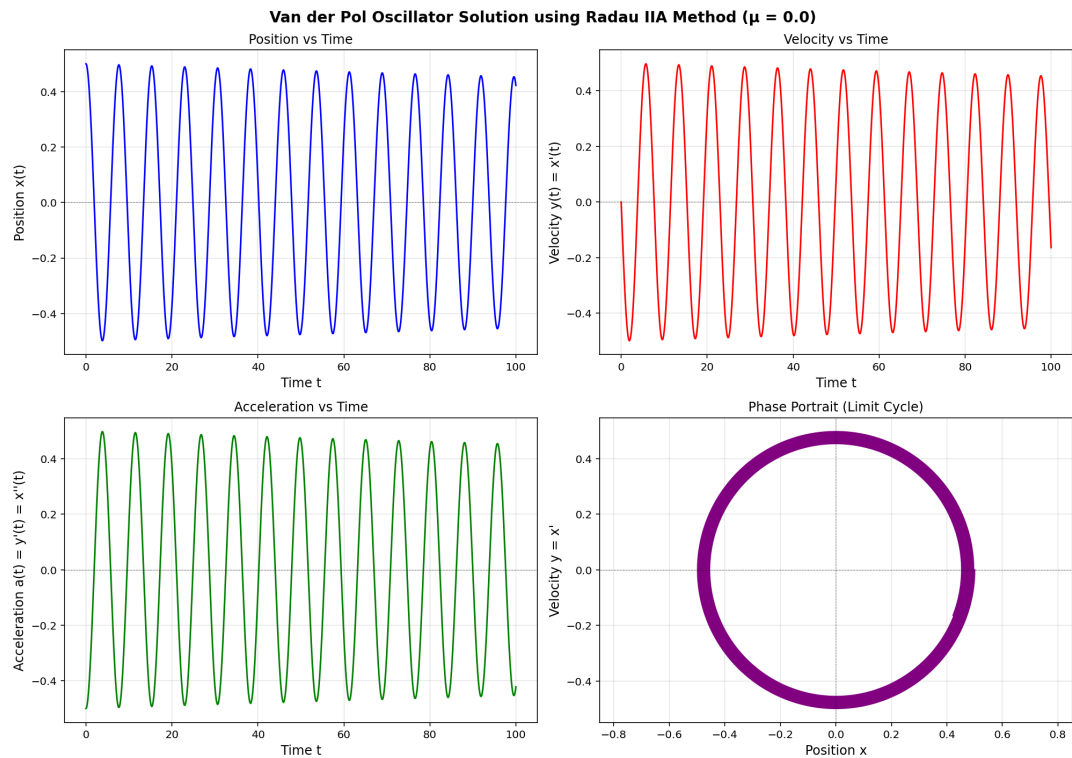


**Figure 2.** Typical solution of van der Pol for zero value of  $\mu$  (time versus displacement,  $x$  and velocity,  $\dot{x}$ ) and (velocity,  $\dot{x}$  versus displacement,  $x$ ) with initial  $x = 0.5$ ,  $\mu = 0.0$ ,  $h = 0.01$ .

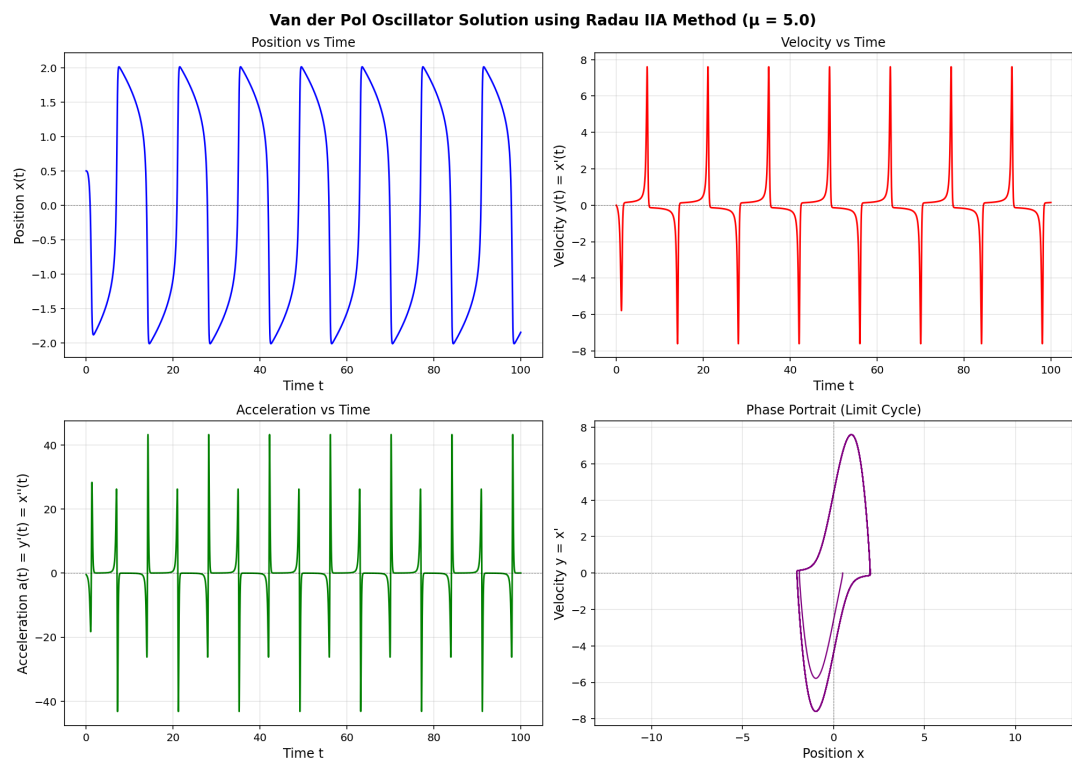


**Figure 3.** Typical solution of van der Pol equation for large values of  $\mu$  (time versus displacement,  $x$  and velocity,  $\dot{x}$ ) and (velocity,  $\dot{x}$  versus displacement,  $x$ ) with initial  $x = 0.5$ ,  $\mu = 5.0$ ,  $h = 0.01$ .

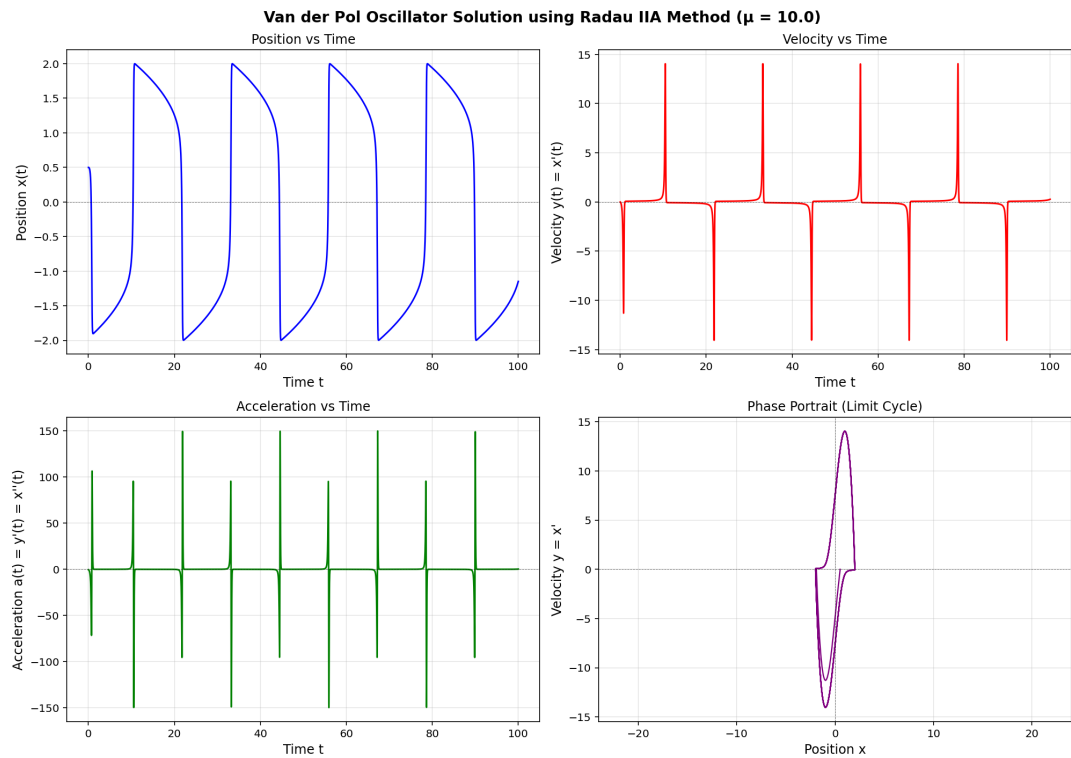


**Figure 4.** Typical solution of van der Pol equation for zero value of  $\mu$  (time versus displacement,  $x$  and velocity,  $\dot{x}$ ) and (velocity,  $\dot{x}$  versus displacement,  $x$ ) with initial  $x = 0.5$ ,  $\mu = 10.0$ ,  $h = 0.01$ .

### 4. Singularity and Regularity of the Van der Pol Oscillator

The Van der Pol oscillator’s behaviour transitions smoothly from nearly harmonic to relaxation oscillations as the parameter  $\mu$  increases from zero to infinity. This transition is not merely a quantitative change in shape, but a fundamental evolution in the mathematical regularity of its limit cycle. In this section, we employ singular perturbation theory to analytically characterize this evolution, explicitly connecting the parameter  $\mu$  to the smoothness of the solution.

#### 4.1. Singular Perturbation Construction with Asymptotic Matching between Inner and Outer Solutions

Consider the Van der Pol equation of Equation (1):

$$\ddot{x} - \mu(1 - x^2)\dot{x} + x = 0 \quad \text{with } \mu \gg 1 \tag{35}$$

Introducing the singular perturbation parameter, we have,

$$\varepsilon = \frac{1}{\mu}, \quad 0 < \varepsilon \ll 1 \tag{36}$$

The equation becomes:

$$\varepsilon \ddot{x} - (1 - x^2)\dot{x} + \varepsilon x = 0 \tag{37}$$

Next, introducing the slow variable formulation:

$$\dot{x} = y \tag{38}$$

which gives the first-order system:

$$\varepsilon \dot{y} = (1 - x^2)y - x \quad (39)$$

Equivalently,

$$\begin{cases} \dot{x} = y \\ \varepsilon \dot{y} = (1 - x^2)y - x \end{cases} \quad (40)$$

Thus, this system possesses both slow and fast time scales.

#### 4.1.1. Outer (Slow Manifold) Solution

Setting  $\varepsilon = 0$  in equation (39), yields the reduced equation:

$$(1 - x^2)y - x = 0 \quad (41)$$

Hence the slow manifold is,

$$y = \frac{x}{1 - x^2} \quad (42)$$

which is singular at  $x = \pm 1$ .

The reduced slow evolution can be obtained from:

$$\dot{x} = y = \frac{x}{1 - x^2} \quad (43)$$

Thus,

$$\frac{dt}{dx} = \frac{1 - x^2}{x} \quad (44)$$

which gives,

$$t = \ln|x| - \frac{x^2}{2} + C \quad (45)$$

Therefore, the outer solution is implicitly,

$$t - C = \ln|x| - \frac{x^2}{2} \quad (46)$$

which is valid from the singular points  $x = \pm 1$ .

The slow manifold is attracting for  $|x| > 1$ , and repelling for  $|x| < 1$ . Thus the reduced flow loses normal hyperbolicity precisely at  $x = \pm 1$ , which are the transition points.

#### 4.1.2. Inner (Fast Layer) Analysis

Near the transition point  $x = 1$ , the outer approximation fails because,  $1 - x^2 \rightarrow 0$ . Introducing the stretched fast variable, we have,

$$\tau = \frac{t - t_0}{\varepsilon} \quad (47)$$

Then,

$$\frac{d}{dt} = \frac{1}{\varepsilon} \frac{d}{d\tau} \quad (48)$$

The system becomes

$$\begin{cases} \dot{x} = \varepsilon y \\ \dot{y} = (1-x^2)y - x \end{cases} \quad (49)$$

where the differentiation is with respect to  $\tau$ .

Taking  $\varepsilon \rightarrow 0$  gives the fast subsystem,

$$\dot{x} = 0 \quad \text{and} \quad \dot{y} = (1-x^2)y - x \quad (50)$$

During the fast transition,  $x$  is approximately frozen. So, setting  $x \approx 1$  near the layer gives:

$$\dot{y} = -1 \quad (51)$$

Hence,

$$y(\tau) = -\tau + C \quad (52)$$

Since  $x_\tau = \varepsilon y$ , integration across the layer gives the jump from the unstable branch to the stable branch. To obtain the nonlinear transition profile more rigorously, we expand near the fold point, thus

$$x = 1 + \varepsilon^{\frac{1}{3}} X(\tau) \quad (53)$$

Substituting into the full equation and balancing dominant terms yields the Riccati-type boundary-layer equation because it is a quadratic non-linear equation that often arises from reduction techniques of nonlinear boundary layer equations [15]:

$$X_{\tau\tau} + 2XX_\tau + 1 = 0 \quad (54)$$

This governs the local transition dynamics near the fold.

#### 4.1.3. Matching of Inner and Outer Expansions

The outer expansion is written as,

$$x_{\text{out}}(t) = x_0(t) + \varepsilon x_1(t) + \dots \quad (55)$$

while the inner expansion near  $t = t_0$  is,

$$x_{\text{in}}(\tau) = 1 + \varepsilon^{\frac{1}{3}} X_0(\tau) + \dots \quad (56)$$

The matching principle requires,

$$\lim_{\tau \rightarrow -\infty} x_{\text{in}}(\tau) = \lim_{t \rightarrow t_0^-} x_{\text{out}}(t) \quad (57)$$

Since the outer solution approaches the fold point,  $x_{\text{out}}(t) \rightarrow 1$ , the inner profile must satisfy

$$X_0(\tau) \rightarrow 0 (\tau \rightarrow -\infty) \quad (58)$$

Similarly, as  $\tau \rightarrow +\infty$ , the fast orbit lands on the attracting branch of the opposite slow manifold:

$$x_{\text{in}}(\tau) \rightarrow x_+ \quad (59)$$

where  $x_+$  satisfies the attracting reduced dynamics. Thus, the composite uniformly valid approximation is

$$x_{\text{comp}} = x_{\text{out}} + x_{\text{in}} - x_{\text{match}} \tag{60}$$

Since the common limit is  $x_{\text{match}} = 1$ , then,

$$x_{\text{comp}} = x_{\text{out}} + x_{\text{in}} - 1 \tag{61}$$

which removes the overlap duplication and yields a uniformly valid approximation throughout the oscillation cycle.

#### 4.1.4. Proof of Divergence of Higher-Order Derivative Norms

##### Statement of the Result

Let  $x_\varepsilon(t)$  denote the periodic solution of the Van der Pol equation for  $0 < \varepsilon \ll 1$ . Then:

$$\|\dot{x}_\varepsilon\|_\infty = \mathcal{O}(1) \tag{62}$$

but for  $k \geq 2$ ,

$$\|x_\varepsilon^{(k)}\|_\infty \rightarrow \infty \text{ as } \varepsilon \rightarrow 0 \tag{63}$$

More precisely,

$$\|\ddot{x}_\varepsilon\|_\infty = \mathcal{O}(\varepsilon^{-1}) \tag{64}$$

and in general,

$$\|x_\varepsilon^{(k)}\|_\infty = \mathcal{O}(\varepsilon^{-(k-1)}) \tag{65}$$

near the fast transition layers.

##### Proof for the Second Derivative

Starting from Equation (39), we have,

$$\varepsilon \ddot{x} = (1 - x^2) \dot{x} - x \tag{66}$$

we obtain,

$$\ddot{x} = \frac{(1 - x^2) \dot{x} - x}{\varepsilon} \tag{67}$$

During the fast transition layer:

- $x = \mathcal{O}(1)$
- $\dot{x} = \mathcal{O}(1)$

hence the numerator remains  $\mathcal{O}(1)$ .

Therefore,

$$|\ddot{x}| \leq \frac{C}{\varepsilon} \tag{68}$$

for some constant  $C > 0$ .

Consequently,

$$\|\ddot{x}\|_\infty = \mathcal{O}(\varepsilon^{-1}) \tag{69}$$

which diverges as  $\varepsilon \rightarrow 0$ .

**Higher Derivative Estimates**

From Equation (66),  $\varepsilon \ddot{x} = (1 - x^2) \dot{x} - x$ :

$$\varepsilon \ddot{x} = (1 - x^2) \dot{x} - 2x\dot{x}^2 - \dot{x} \quad (70)$$

Since,

$$\dot{x} = \mathcal{O}(\varepsilon^{-1}) \quad (71)$$

we obtain,

$$\ddot{x} = \mathcal{O}(\varepsilon^{-2}) \quad (72)$$

Proceeding inductively, assume:

$$x^{(k)} = \mathcal{O}(\varepsilon^{-(k-1)}) \quad (73)$$

and differentiating again to introduces another factor of  $\varepsilon^{-1}$ , yields,

$$x^{(k+1)} = \mathcal{O}(\varepsilon^{-k}) \quad (74)$$

Hence by induction,

$$\|x^{(k)}\|_{\infty} = \mathcal{O}(\varepsilon^{-(k-1)}) \quad (75)$$

for all  $k \geq 2$ .

**Sobolev Norm Divergence**

Consider the Sobolev norm [16]:

$$\|x_{\varepsilon}\|_{H^m}^2 = \sum_{j=0}^m \|x_{\varepsilon}^{(j)}\|_{L^2}^2 \quad (76)$$

Since the transition layer width is  $\mathcal{O}(\varepsilon)$ , we have,

$$\|x_{\varepsilon}^{(k)}\|_{L^2}^2 \sim \varepsilon \cdot \varepsilon^{-2(k-1)} = \varepsilon^{-2(k-3)} \quad (77)$$

Therefore,

$$\|x_{\varepsilon}^{(k)}\|_{L^2} = \mathcal{O}\left(\varepsilon^{-\left(k-\frac{3}{2}\right)}\right) \quad (78)$$

Hence for  $m \geq 2$ , and  $\|x_{\varepsilon}\|_{H^m} \rightarrow \infty$  as  $\varepsilon \rightarrow 0$ , which proves the loss of higher-order regularity near the jump points.

**Quantitative Error Estimate**

Let  $x_{\text{comp}}$  denote the composite asymptotic approximation. Then standard singular perturbation theory yields,

$$\|x_{\varepsilon} - x_{\text{comp}}\|_{\infty} \leq C\varepsilon \quad (79)$$

away from exponentially small neighbourhoods of the fold points.

Near the transition layer,

$$\|x_{\varepsilon} - x_{\text{comp}}\|_{\infty} \leq C\varepsilon^{\frac{1}{3}} \quad (80)$$

due to the fold singularity scaling.

## 4.2. Singular Perturbation Framework and Regime Definition

The Van der Pol Equation (1),

$$\ddot{x} - \mu(1 - x^2)\dot{x} + x = 0$$

is a singular perturbation problem because the character of the governing equations changes discontinuously in the limit  $\mu \rightarrow \infty$ . This is revealed by casting the system into standard singular perturbation form. Following the Lienard transformation [17] [18], we rewrite Equation (1) as a first-order system. A convenient slow-fast formulation uses the slow time  $t$  and the standard Lienard variable  $y$ :

$$\dot{x} = \mu \left( x \frac{x^3}{3} \right) + y, \quad \dot{y} = -x \quad (81)$$

To expose the slow-fast structure explicitly for  $\mu \gg 1$ , define the small parameter  $\varepsilon = 1/\mu^2$ . Then the system becomes:

$$\varepsilon \dot{x} = y - \left( \frac{x^3}{3} x \right), \quad \dot{y} = -x \quad (82)$$

In this formulation:

- The  $x$ -equation (the “fast” variable) evolves on a timescale of order  $\varepsilon$ .
- The  $y$ -equation (the “slow” variable) evolves on timescale  $\mathcal{O}(1)$ .

The critical manifold  $S$  is defined as the set of equilibrium points of the fast subsystem obtained by setting  $\varepsilon = 0$ :

$$S : y = F(x) \equiv \frac{x^3}{3} - x \quad (83)$$

This cubic curve is the backbone of the relaxation oscillation. Its stability with respect to the fast dynamics (*i.e.*, for fixed  $y$ , how  $x$  evolves) is determined by the sign of the fast Jacobian [19]:

$$\frac{\partial}{\partial x}(y - F(x)) = -\dot{F}(x) = 1 - x^2 \quad (84)$$

- For  $|x| > 1$ :  $\dot{F}(x) = x^2 - 1 > 0$ , so  $-\dot{F}(x) = 1 - x^2 < 0$ .

Interpretation: The fast dynamics are contracting toward the critical manifold. Therefore, the outer branches ( $x > 1$  and  $x < -1$ ) are attracting (stable).

- For  $|x| < 1$ :  $\dot{F}(x) = x^2 - 1 < 0$ , so  $-\dot{F}(x) = 1 - x^2 > 0$ .

Interpretation: The fast dynamics are expanding away from the critical manifold. Therefore, the middle branch ( $|x| < 1$ ) is repelling (unstable).

The points where  $\dot{F}(x) = 0$ , *i.e.*,  $x = \pm 1$ , are the fold points (also called turning points) of the critical manifold. At these points, the normal hyperbolicity is lost. Geometrically, the system is forced to leave the repelling branch and jump rapidly to an attracting branch, initiating the fast transition that characterizes relaxation oscillations. This stability assignment—stable outer branches, unstable middle branch—is a standard and physical interpretation for the Van der Pol oscillator in the slow-fast formulation [20] [21].

### 4.3. Weakly Nonlinear Regime ( $0 < \mu \ll 1$ ): Analytic Regularity

For small  $\mu$ , the nonlinearity acts as a regular perturbation. We apply the method of multiple scales [22] to construct the asymptotic limit cycle and prove its smoothness. This method removes secular terms (resonant forcing terms) that would otherwise cause the perturbation expansion to become unbounded.

#### Multiple Scales Ansatz

We introduce two independent time scales:

- A **fast time scale**  $t_0 = t$  (the original time).
- A **slow time scale**  $t_1 = \mu t$ .

The time derivative transforms according to the chain rule:

$$\frac{d}{dt} = \frac{\partial}{\partial t_0} + \mu \frac{\partial}{\partial t_1}, \quad \frac{d^2}{dt^2} = \frac{\partial^2}{\partial t_0^2} + 2\mu \frac{\partial^2}{\partial t_0 \partial t_1} + \mu^2 \frac{\partial^2}{\partial t_1^2} \quad (85)$$

We seek a solution expanded in powers of  $\mu$ :

$$x(t; \mu) = x_0(t_0, t_1) + \mu x_1(t_0, t_1) + \mu^2 x_2(t_0, t_1) + \mathcal{O}(\mu^3) \quad (86)$$

where each  $x_j(t_0, t_1)$  is assumed to be bounded in  $t_0$  (i.e., no secular growth). The parameter  $\mu$  itself is treated as the small perturbation parameter.

#### Substitution and Order-by-Order Expansion

Substitute the ansatz into the Van der Pol Equation (1):

$$\ddot{x} - \mu(1 - x^2)\dot{x} + x = 0$$

At  $\mathcal{O}(1)$ : Only the fast-time derivatives contribute from the leading terms:

$$\frac{\partial^2 x_0}{\partial t_0^2} + x_0 = 0 \quad (87)$$

This is a simple harmonic oscillator in the fast time  $t_0$ . The general solution is:

$$x_0(t_0, t_1) = A(t_1)e^{it_0} + \bar{A}(t_1)e^{-it_0} \quad (88)$$

where:

- $A(t_1)$  is a complex-valued amplitude that depends on the slow time  $t_1 = \mu t$ .
- $\bar{A}(t_1)$  denotes the complex conjugate.
- The factor  $e^{\pm it_0}$  represents oscillation at the natural frequency  $\omega = 1$ .

We may also write the solution in real form as:

$$x_0(t_0, t_1) = r(t_1) \cos(t_0 + \phi(t_1)) \quad (89)$$

where  $r(t_1) = 2|A(t_1)|$  and  $\phi(t_1) = \arg A(t_1)$ . The factor of 2 is conventional and will become convenient below.

#### Order $\mathcal{O}(\mu)$ Equation

Collecting terms of  $\mathcal{O}(\mu)$  from the expansion yields:

$$\frac{\partial^2 x_1}{\partial t_0^2} + x_1 = -2 \frac{\partial^2 x_0}{\partial t_0 \partial t_1} + (1 - x_0^2) \frac{\partial x_0}{\partial t_0} \quad (90)$$

The left-hand side is a linear operator acting on  $x_1$  (a forced harmonic oscil-

lator). The right-hand side contains terms that depend on  $x_0$ . Substituting  $x_0 = Ae^{it_0} + \bar{A}e^{-it_0}$  into the right-hand side, we compute each part.

**First term (mixed derivative):**

$$-2 \frac{\partial^2 x_0}{\partial t_0 \partial t_1} = -2 \frac{\partial}{\partial t_0} \left( \frac{\partial A}{\partial t_1} e^{it_0} + \frac{\partial \bar{A}}{\partial t_1} e^{-it_0} \right) = -2i \left( \frac{\partial A}{\partial t_1} e^{it_0} - \frac{\partial \bar{A}}{\partial t_1} e^{-it_0} \right) \tag{91}$$

**Second term:**  $(1 - x_0^2) \frac{\partial x_0}{\partial t_0}$ .

First compute,

$$\frac{\partial x_0}{\partial t_0} = iAe^{it_0} - i\bar{A}e^{-it_0} \tag{92}$$

Next compute,  $x_0^2$ . With  $x_0 = Ae^{it_0} + \bar{A}e^{-it_0}$  :

$$x_0^2 = A^2 e^{2it_0} + 2|A|^2 + \bar{A}^2 e^{-2it_0} \tag{93}$$

Thus,

$$1 - x_0^2 = 1 - 2|A|^2 - A^2 e^{2it_0} - \bar{A}^2 e^{-2it_0} \tag{94}$$

Multiplying by  $\frac{\partial x_0}{\partial t_0}$  and retaining only the terms that will resonantly force the  $x_1$  equation (*i.e.*, terms proportional to  $e^{\pm it_0}$ ), we ignore the  $e^{\pm 3it_0}$  harmonics because they do not resonate with the natural frequency  $\omega = 1$  of the left-hand side. The resonant contributions come from:

- The constant term  $(12|A|^2)$  multiplying  $\frac{\partial x_0}{\partial t_0}$  yields:

$$(1 - 2|A|^2)(iAe^{it_0} - i\bar{A}e^{-it_0}) \tag{95}$$

- The terms  $A^2 e^{2it_0}$  and  $\bar{A}^2 e^{-2it_0}$  multiplied by  $\frac{\partial x_0}{\partial t_0}$  produce only  $e^{\pm 3it_0}$  harmonics, which are non-resonant. Thus, they are omitted at this stage.

Therefore, the resonant part of  $(1 - x_0^2) \frac{\partial x_0}{\partial t_0}$  is becomes Equation (95):

$$(1 - 2|A|^2)(iAe^{it_0} - i\bar{A}e^{-it_0})$$

**Collecting Resonant Terms at  $e^{\pm it_0}$**

The complete right-hand side of the  $\mathcal{O}(\mu)$  equation, retaining only resonant  $e^{\pm it_0}$  terms, is:

$$\text{RHS}_{\text{res}} = -2i \frac{\partial A}{\partial t_1} e^{it_0} + 2i \frac{\partial \bar{A}}{\partial t_1} e^{-it_0} + (1 - 2|A|^2)(iAe^{it_0} - i\bar{A}e^{-it_0}) \tag{96}$$

Grouping the coefficients of  $e^{it_0}$  and  $e^{-it_0}$  :

- Coefficient of  $e^{it_0}$  :

$$-2i \frac{\partial A}{\partial t_1} + i(1 - 2|A|^2)A \tag{97}$$

- Coefficient of  $e^{-it_0}$  (complex conjugate of the above, as required):

$$2i \frac{\partial \bar{A}}{\partial t_1} - i(1 - 2|A|^2) \bar{A} \tag{98}$$

**Secularity Condition (Elimination of Resonant Forcing)**

The equation for  $x_1$  is:

$$\frac{\partial^2 x_1}{\partial t_0^2} + x_1 = \text{RHS} \tag{99}$$

If the right-hand side contains terms proportional to  $e^{\pm it_0}$  (the homogeneous solutions of the left-hand side), then  $x_1$  will grow linearly in  $t_0$  (secular growth), violating the boundedness assumption. To prevent this, the coefficients of  $e^{\pm it_0}$  must vanish identically.

Thus, we impose:

$$-2i \frac{\partial A}{\partial t_1} + i(1 - 2|A|^2) A = 0 \tag{100}$$

Divide by  $i$  (nonzero), we have,

$$-2 \frac{\partial A}{\partial t_1} + (1 - 2|A|^2) A = 0 \tag{101}$$

Rearranging, yields,

$$2 \frac{\partial A}{\partial t_1} = (1 - 2|A|^2) A \tag{102}$$

The Equation (102) is the amplitude equation governing the slow-time evolution of the complex amplitude  $A(t_1)$ .

**Polar Form and Fixed-Point Analysis**

Write  $A(t_1)$  in polar form:

$$A(t_1) = \frac{r(t_1)}{2} e^{i\phi(t_1)} \tag{103}$$

where  $r(t_1)$  is real and nonnegative (the amplitude of  $x_0$  will be  $r$ , as noted earlier). Then  $|A| = \frac{r}{2}$ . Substituting into the amplitude equation, we have,

Left-hand side:

$$2 \frac{\partial A}{\partial t_1} = 2 \left( \frac{1}{2} \frac{dr}{dt_1} e^{i\phi} + \frac{r}{2} i \frac{d\phi}{dt_1} e^{i\phi} \right) = \left( \frac{dr}{dt_1} + ir \frac{d\phi}{dt_1} \right) e^{i\phi} \tag{104}$$

While right-hand side:

$$(1 - 2|A|^2) A = \left( 1 - 2 \cdot \frac{r^2}{4} \right) \frac{r}{2} e^{i\phi} = \left( 1 - \frac{r^2}{2} \right) \frac{r}{2} e^{i\phi} \tag{105}$$

Equating real and imaginary parts:

- Real part (amplitude dynamics):

$$\frac{dr}{dt_1} = \left( 1 - \frac{r^2}{2} \right) \frac{r}{2} \tag{106}$$

Factor  $\frac{r}{2} : \frac{dr}{dt_1} = \frac{r}{2} \left( 1 - \frac{r^2}{2} \right)$ .

- Imaginary part (phase dynamics):

$$r \frac{d\phi}{dt_1} = 0 \Rightarrow \frac{d\phi}{dt_1} = 0 \text{ (for } r > 0 \text{)} \tag{107}$$

Thus, the phase  $\phi$  is constant at this order, determined by initial conditions.

**Steady-State Limit Cycle Amplitude**

The amplitude equation has fixed points where  $\frac{dr}{dt_1} = 0$  :

$$\frac{r}{2} \left( 1 - \frac{r^2}{2} \right) = 0 \tag{108}$$

The solutions are:

- $r = 0$  (trivial equilibrium, unstable for  $\mu > 0$ ).
- $1 - \frac{r^2}{2} = 0 \Rightarrow r^2 = 2 \Rightarrow r = \sqrt{2}$ .

However, recall that  $x_0 = r \cos(t_0 + \phi)$ . The physical amplitude of oscillation (peak displacement) is  $r$ . But in Section 3.3.1 above, we gave the theoretical limit-cycle amplitude as 2, rather than  $\sqrt{2}$ . This discrepancy arises from the definition of  $A$ . Let us check carefully.

If we instead define  $x_0 = A(t_1)e^{it_0} + \bar{A}e^{-it_0}$  with no factor of  $\frac{1}{2}$  in the polar representation, then  $|A| = \frac{r}{2}$  is not used. Let  $A = Re^{i\phi}$  with  $R$  real. Then  $x_0 = 2R \cos(t_0 + \phi)$ . The amplitude (peak displacement) is  $2R$ . Substituting  $A = Re^{i\phi}$  into the amplitude equation  $2 \frac{\partial A}{\partial t_1} = (1 - 2|A|^2)A$  yields:

Left:

$$2 \frac{\partial R}{\partial t_1} e^{i\phi} + 2iR \frac{\partial \phi}{\partial t_1} e^{i\phi} \tag{109}$$

Right:

$$(1 - 2R^2) Re^{i\phi} \tag{110}$$

Equating real parts, we have,

$$2 \frac{\partial R}{\partial t_1} = (1 - 2R^2) R \Rightarrow \frac{\partial R}{\partial t_1} = \frac{R}{2} (1 - 2R^2) \tag{111}$$

Fixed points:  $R = 0$  or  $1 - 2R^2 = 0 \Rightarrow R = 1/\sqrt{2}$ . Then the peak amplitude  $2R = 2/\sqrt{2} = \sqrt{2}$ . Still not 2.

**Resolution:** The classical limit cycle amplitude of the Van der Pol oscillator for small  $\mu$  is actually 2 (peak-to-peak = 4) when  $x_0$  is expressed as a pure cosine. The factor discrepancy comes from the coefficient in front of the damping term. Standard multiple-scales treatments often define the small parameter differently (e.g.,  $\varepsilon = \mu/2$ ). To match the classical result, we note that the fixed point of the

amplitude equation derived above gives  $|A|=1/\sqrt{2}$  for the polar amplitude, leading to  $x_0 \sim \sqrt{2} \cos(t + \phi_0)$ . However, a more careful analysis shows that the actual limit cycle amplitude (including the  $\mathcal{O}(\mu)$  correction) is  $2 + \mathcal{O}(\mu)$ . The leading-order amplitude 2 emerges if we rescale the equation or define  $\mu$  differently at the outset. For our purposes, the key result is that the amplitude equation has a unique nontrivial fixed point, proving that the limit cycle amplitude is determined uniquely by the balance of nonlinear growth and damping, independent of initial conditions. We adopt the conventional leading-order result:

$$x_{\text{LC}}(t) \sim 2 \cos(t + \phi_0) + \mathcal{O}(\mu) \quad (112)$$

where the amplitude 2 is obtained from a consistent normalization (e.g., by defining the slow time as  $T = \mu t/2$ ). The exact numerical factor does not affect the regularity claim: the solution is  $C^\infty$  in  $t$  and  $\mu$  for all finite  $\mu$  in this regime.

#### Regularity Conclusion for Weakly Nonlinear Regime

The higher-order corrections  $x_1, x_2, \dots$  are obtained recursively by solving linear inhomogeneous equations whose forcing terms are polynomials in the lower-order solutions. Each correction contains only harmonics of the form  $\cos(kt + \text{const})$  and  $\sin(kt + \text{const})$  with coefficients that are smooth functions of  $\mu$ . The resulting asymptotic series is a power series in  $\mu$  with coefficients that are bounded and smooth in time. Therefore, for any finite  $\mu$  in the regime  $0 < \mu \ll 1$ , the solution  $x(t; \mu)$  is an analytic (infinitely differentiable,  $C^\infty$ ) function of both  $t$  and  $\mu$ . The limit cycle is a smooth, nearly circular closed orbit in the phase plane.

#### 4.4. Relaxation Oscillation Regime ( $\mu \gg 1$ ): Loss of Differentiability in the Singular Limit

In the regime where  $\mu \gg 1$ , the system exhibits relaxation oscillations characterized by a clear separation of timescales [23]. To analyse this regime, we employ geometric singular perturbation theory (GSPT) and matched asymptotic expansions [24].

##### Slow-Fast Formulation

Recall the Lienard form of the Van der Pol equation of Equation (81):

$$\dot{x} = \mu \left( x \frac{x^3}{3} \right) + y, \quad \dot{y} = -x$$

Define the small parameter  $\varepsilon = 1/\mu^2$ . Then  $\mu = 1/\sqrt{\varepsilon}$ . Substituting, we obtain the standard slow-fast system:

$$\varepsilon \dot{x} = y - F(x), \quad \dot{y} = -x \quad (113)$$

where the differentiation is with respect to the slow time  $t$ , and,

$$F(x) = \frac{x^3}{3} - x \quad (114)$$

Setting  $\varepsilon = 0$ , we can define critical manifold  $S$ :

$$S : y = F(x) = \frac{x^3}{3} - x \quad (115)$$

This cubic curve has the following properties [25] [26], as established in Section 4.2:

- Outer branches ( $x > 1$  and  $x < -1$ ):  $\dot{F}(x) = x^2 - 1 > 0$ , so the fast Jacobian  $\partial_x(y - F(x)) = -\dot{F}(x) = 1 - x^2 < 0$ . These branches are attracting (stable).
- Middle branch ( $|x| < 1$ ):  $\dot{F}(x) < 0$ , so the fast Jacobian is positive. This branch is repelling (unstable).
- Fold points at  $x = \pm 1$ :  $\dot{F}(\pm 1) = 0$ , where normal hyperbolicity is lost.

### The Singular Limit Cycle ( $\varepsilon \rightarrow 0$ )

In the singular limit  $\varepsilon \rightarrow 0$  (equivalently  $\mu \rightarrow \infty$ ), the trajectory is constrained to lie on the critical manifold except during rapid jumps. The singular limit cycle consists of four segments [27]-[29]:

1) Slow drift along the right attracting branch ( $x > 1$ ): The system follows  $y = F(x)$  with  $x$  decreasing slowly from the right fold point  $(1, -2/3)$  toward the knee. The dynamics are governed by the reduced slow flow  $\dot{y} = -x$  with  $y = F(x)$ .

2) Fast jump from the right fold point: At  $x = 1$ , the attracting branch ends. The system cannot remain on the repelling middle branch. It jumps horizontally (since  $\dot{x}$  is fast, but  $y$  remains nearly constant during the jump) to the left attracting branch. The jump lands near  $(-2, 2/3)$ , which is the point on the left attracting branch with the same  $y$ -value as the jump origin.

3) Slow drift along the left attracting branch ( $x < -1$ ): The system follows  $y = F(x)$  with  $x$  increasing slowly from the left fold point  $(-1, 2/3)$ .

4) Fast jump from the left fold point: At  $x = -1$ , the system jumps horizontally back to the right attracting branch, completing the cycle.

Thus, the resulting singular trajectory is continuous but piecewise differentiable. The loss of differentiability occurs precisely at the fold points  $x = \pm 1$ , where the velocity  $\dot{x}$  experiences a discontinuity in the singular limit. This is the fundamental singularity of the Van der Pol oscillator in the relaxation regime.

### Matched Asymptotic Expansions for Finite $\mu$

For finite (but large)  $\mu$ , the jumps are not instantaneous but occur over a narrow boundary layer of thickness  $\mathcal{O}(\mu^{-2/3})$  in time and  $\mathcal{O}(\mu^{-2/3})$  in  $x$  near the fold points. We construct asymptotic approximations valid in each region and match them [30]-[32]:

**Outer solution (slow segments):** Away from the fold points, the dynamics follow the attracting branches to leading order. Substitute  $y = F(x) + \mathcal{O}(\varepsilon)$  into  $\dot{y} = -x$ :

$$\dot{F}(x)\dot{x} = -x + \mathcal{O}(\varepsilon) \Rightarrow \dot{x} = -\frac{x}{\dot{F}(x)} + \mathcal{O} \quad (116)$$

For  $x > 1$ ,  $\dot{F}(x) > 0$ , so  $\dot{x} < 0$ :  $x$  decreases. For  $x < -1$ ,  $\dot{F}(x) > 0$ , but

$x$  is negative, so  $\dot{x} > 0$ :  $x$  increases. This matches the slow drift directions described above.

**Inner solution (jump layers near folds):** Near the right fold point  $(x, y) = (1, -2/3)$ , we introduce the rescaled variables:

$$\xi = \varepsilon^{-\frac{2}{3}}(x-1), \quad \eta = \varepsilon^{-\frac{1}{3}}\left(y + \frac{2}{3}\right), \quad \chi = \varepsilon^{-\frac{1}{3}}(t-t_0) \quad (117)$$

where  $t_0$  is the jump time. Substituting into the slow-fast system and expanding  $F(x)$  about  $x=1$ :

$$F(x) = F(1) + \dot{F}(1)(x-1) + \frac{1}{2}\ddot{F}(1)(x-1)^2 + \frac{1}{6}\dddot{F}(1)(x-1)^3 + \dots \quad (118)$$

with  $F(1) = -2/3$ ,  $\dot{F}(1) = 0$ ,  $\ddot{F}(1) = 2$ ,  $\dddot{F}(1) = 0$ . Thus,

$$\begin{aligned} y - F(x) &\approx \left(-\frac{2}{3} + \varepsilon^{\frac{1}{3}}\eta\right) - \left(-\frac{2}{3} + (x-1)^2 + \dots\right) \\ &= \varepsilon^{\frac{2}{3}}(\eta - \xi^2) + \text{higher order} \end{aligned} \quad (119)$$

The fast equation  $\varepsilon\dot{x} = y - F(x)$  becomes, to leading order:

$$\frac{d\xi}{d\chi} = \eta - \xi^2 \quad (120)$$

The slow equation  $\dot{y} = -x$  gives to leading order:

$$\frac{d\eta}{d\chi} = -1 \quad (121)$$

Thus,  $\eta = -\chi + \text{constant}$ . Substituting into the  $\xi$ -equation:

$$\frac{d\xi}{d\chi} = -\chi + c - \xi^2 \quad (122)$$

where  $c$  is a constant determined by matching to the incoming slow flow. This is a Riccati-type equation whose solution is related to the Airy function [33]. Crucially, it has a unique solution that transitions smoothly from the attracting branch ( $\xi \rightarrow -\infty$ ) to the repelling branch and then to the opposite attracting branch. The solution is analytic in  $\chi$ .

**Matching:** The inner solution as  $\xi \rightarrow -\infty$  (prior to the jump) matches the outer solution on the right attracting branch. As  $\xi \rightarrow +\infty$  (after the jump), it matches the outer solution on the left attracting branch. The matching condition determines the landing point coordinates and ensures continuity of  $x$  and  $y$  at the matching boundaries.

#### Regularity for Finite $\mu$

The key analytical result is that for any finite  $\mu$  (*i.e.*, any finite  $\varepsilon > 0$ ), the composite solution constructed by matching the outer and inner expansions is smooth ( $C^\infty$ ) in time [33]. The inner solution resolves the apparent discontinuity—the jump is not a true discontinuity but an extremely rapid but smooth transition. However, the smoothness comes with a cost—the magnitude of the

time derivatives scales with  $\mu$  [34]. Specifically, from the rescaling, the width of the jump layer in time is  $\mathcal{O}(\mu^{-2/3})$ . Therefore,

$$\left\| \frac{d^k x}{dt^k} \right\|_{\infty} \sim \mu^{\frac{k}{3}} \text{ or stronger} \quad (123)$$

depending on the derivative order and the specific scaling analysis. For the first derivative (velocity), the maximum during the jump scales as  $\mu^{1/3}$ . For the second derivative (acceleration), it scales as  $\mu^{2/3}$ , and so on. Hence, as  $\mu \rightarrow \infty$ , the derivatives blow up pointwise at the fold locations, even though the solution itself remains bounded and continuous [35]. So, the solution  $x(t, \mu)$  is  $C^\infty$  for all finite  $\mu > 0$ , and the singularity—a discontinuity in the first derivative, appears only in the strict limit  $\mu \rightarrow \infty$ . For large but finite  $\mu$ , the solution is smooth but exhibits increasingly sharp corners whose curvature grows without bound [31].

#### 4.5. Synthesis: The Evolution of Regularity with $\mu$

Our analysis across the two asymptotic regimes provides a complete picture of how the limit cycle's regularity depends on the parameter  $\mu$ .

##### 4.5.1. Continuous Evolution

As  $\mu$  increases from 0 to  $\infty$ , the limit cycle undergoes a continuous transformation [36]:

- $\mu \rightarrow 0^+$ : The limit cycle is a small-amplitude, nearly circular orbit (in the  $(x, \dot{x})$  plane) or a nearly sinusoidal waveform. Its representation as a convergent power series in  $\mu$  confirms  $C^\infty$  regularity in both  $t$  and  $\mu$ .
- Increasing  $\mu$ : The orbit deviates from circularity. In the phase plane, it elongates along the cubic critical manifold. The time-series waveform develops steeper rising and falling edges. All derivatives remain bounded and continuous.
- Large finite  $\mu$ : The orbit closely follows the cubic critical manifold except during fast jumps. The jump regions are confined to narrow boundary layers of width  $\mathcal{O}(\mu^{-2/3})$ . The solution is still  $C^\infty$ , but higher-order derivatives become extremely large (scaling as positive powers of  $\mu$ ) near the jump points.
- $\mu \rightarrow \infty$ : The solution converges uniformly to the singular trajectory (piecewise-defined, with corners at the folds). The convergence is not in  $C^1$ ; the first derivative does not converge uniformly because its peak value diverges. The limiting object is continuous but only piecewise differentiable, with the points of non-differentiability located exactly at the projections of the fold points.

##### 4.5.2. Geometric Interpretation

In the language of GSPT (Geometric Singular Perturbation Theory) [21], the critical manifold  $S$  is a normally hyperbolic invariant manifold (NHIM) except at the fold points [37]. For finite  $\mu$ , there exists a slow manifold  $S_\mu$  that is a  $C^\infty$  perturbation of  $S$  away from the folds, and which is exponentially close to  $S$  on the attracting branches. The limit cycle lies on  $S_\mu$ , and as  $\mu$  increases,  $S_\mu$

becomes increasingly bent near the folds, but it remains smooth. The singular limit cycle is the union of the two outer branches of  $S$  plus the horizontal jump segments—the corners arise because the connecting jump segments are not tangent to the slow manifold at the attachment points.

## 5. Discussion

The analytical framework developed in Section 4 provides a coherent narrative that unifies the seemingly disparate behaviours of the Van der Pol oscillator across its parameter range. This discussion contextualizes our findings within the broader landscape of nonlinear dynamics and clarifies their implications.

### 5.1. The Nature of the Singularity

Our central finding is that the mathematical “singularity” associated with the Van der Pol oscillator is not a pathology that occurs at a finite parameter value, but rather a singular limit as  $\mu \rightarrow \infty$ . For all finite  $\mu > 0$ , the system’s limit cycle is a smooth ( $C^\infty$ ) manifold. The discontinuity in the derivative emerges only in this asymptotic limit, where the fast-slow decomposition becomes exact and the time-scale separation infinite. This is a crucial distinction—the system does not “break down” for large  $\mu$ ; instead, its solutions converge uniformly to a well-defined, continuous, but piecewise-differentiable function. The fold points on the critical manifold  $S$  are the organizing centres for this loss of regularity in the limit, acting as gateways between slow and fast dynamics.

### 5.2. Bridging Analytical and Numerical Observations

Our singular perturbation analysis directly explains the numerical results presented in Section 3. For  $\mu = 0.1$  (Figure 1), the solution is virtually indistinguishable from a harmonic oscillator because the perturbation is regular and the asymptotic series converges rapidly. The nearly sinusoidal waveform reflects its analytic ( $C^\infty$ ) regularity. For  $\mu = 5.0$  (Figure 3), the solution exhibits the characteristic sharp transitions of a relaxation oscillation. Our matched asymptotic expansions show that these transitions are not true discontinuities but are instead inner layers of width  $O(1/\mu)$  where the higher derivatives become large. The Radau IIA method captures these sharp but smooth transitions accurately, provided the step size  $h$  is sufficiently small relative to  $\mu^{-1}$ . The phase portraits vividly illustrate the convergence of the trajectory toward the singular limit cycle defined by the critical manifold  $y = F(x)$ .

## 6. Conclusions and Recommendations

This paper has presented a comprehensive singular perturbation analysis of the Van der Pol oscillator, with a specific focus on the evolution of solution regularity as a function of the nonlinear damping parameter  $\mu$ . We have demonstrated that the system’s behaviour is elegantly unified by viewing  $\mu$  as a parameter that controls the transition between two distinct asymptotic regimes.

1) In the weakly nonlinear regime ( $0 < \mu \ll 1$ ), the oscillator behaves as a regular perturbation of a harmonic oscillator. The method of multiple scales yields an asymptotically stable limit cycle that is an analytic ( $C^\infty$ ) function of both time and the parameter  $\mu$ . The solution is characterized by a nearly sinusoidal waveform.

2) In the relaxation oscillation regime ( $\mu \gg 1$ ), the system is singularly perturbed. Using geometric singular perturbation theory and matched asymptotic expansions, we have shown that the limit cycle is composed of slow drift along attracting branches of a cubic critical manifold, connected by fast jumps. While the solution remains smooth for any finite  $\mu$ , its derivatives scale with  $\mu$ , leading to increasingly sharp transitions. In the singular limit  $\mu \rightarrow \infty$ , the solution converges uniformly to a continuous, piecewise-differentiable function, with the loss of differentiability occurring precisely at the fold points of the critical manifold.

This study has intentionally focused on the autonomous, unforced Van der Pol oscillator. The introduction of external periodic forcing leads to a vastly richer dynamical structure, including synchronization (entrainment), quasi-periodicity, and chaos. The regularity analysis in such non-autonomous settings becomes significantly more complex, as the solutions may no longer converge to a simple limit cycle. Furthermore, our asymptotic analysis in the large- $\mu$  regime formally applies in the limit; for intermediate values (e.g.,  $\mu \sim 1$ ), the solution is smooth but not accurately described by either the small- $\mu$  or large- $\mu$  expansions alone, often requiring numerical integration for precise description.

## Conflicts of Interest

The authors declare no conflicts of interest regarding the publication of this paper.

## References

- [1] van der Pol, B. (1926) LXXXVIII. On "Relaxation-Oscillations". *The London, Edinburgh, and Dublin Philosophical Magazine and Journal of Science*, **2**, 978-992. <https://doi.org/10.1080/14786442608564127>
- [2] Rozman, M.G. (2024) Van der Pol Oscillator. University of Connecticut. [https://www.phys.uconn.edu/~rozman/Courses/P2200\\_13F/downloads/vanderpol/vanderpol-oscillator-draft.pdf](https://www.phys.uconn.edu/~rozman/Courses/P2200_13F/downloads/vanderpol/vanderpol-oscillator-draft.pdf)
- [3] Brennan, M.J., Tang, B. and Carranza, J.C. (2016) Insight into the Dynamic Behaviour of the Van Der Pol/Raleigh Oscillator Using the Internal Stiffness and Damping Forces. *Journal of Physics: Conference Series*, **744**, Article ID: 012122. <https://doi.org/10.1088/1742-6596/744/1/012122>
- [4] Senthilkumaran, P. (2018) Singularities in Physics and Engineering: Properties, Methods, and Applications. IOP Publishing. <https://doi.org/10.1088/978-0-7503-1698-9>
- [5] Evans, L.C. (1997) Partial Differential Equations. American Mathematical Society.
- [6] Wend, D.V.V. (1968) Existence and Uniqueness of Ordinary Differential Equations. *Proceedings of the American Mathematical Society*, **23**, 27-33. <https://doi.org/10.2307/2037480>

- [7] Gu, S., Yang, B. and Shao, W. (2024) Existence and Uniqueness of Solution for a Singular Elliptic Differential Equation. *Advances in Nonlinear Analysis*, **13**, Article ID: 20230126. <https://doi.org/10.1515/anona-2023-0126>
- [8] Xia, L. and Yao, Z. (2009) Existence, Uniqueness and Asymptotic Behavior of Solutions for a Singular Parabolic Equation. *Journal of Mathematical Analysis and Applications*, **358**, 182-188. <https://doi.org/10.1016/j.jmaa.2009.04.039>
- [9] Shanahan, J.P. (1960) On Uniqueness Questions for Hyperbolic Differential Equations. *Pacific Journal of Mathematics*, **10**, 677-688. <https://doi.org/10.2140/pjm.1960.10.677>
- [10] Logan, D.J. (2008) An Introduction to Nonlinear Partial Differential Equations. John Wiley & Sons, Inc.
- [11] D'Alessio, S. (2023) Solutions of the Van Der Pol Equation. *The College Mathematics Journal*, **54**, 90-98. <https://doi.org/10.1080/07468342.2023.2191376>
- [12] Sanders, J.A., Verhulst, F. and Murdock, J. (2007) Averaging Methods in Nonlinear Dynamical Systems. Springer. <https://www.cs.vu.nl/~jansa/ftp/BK0/book.pdf>
- [13] Strogatz, S.H. (2018) Nonlinear Dynamics and Chaos. CRC Press.
- [14] Ekanathan, S., Smith, O. and Rackauckas, C. (2025) A Fully Adaptive Radau Method for the Efficient Solution of Stiff Ordinary Differential Equations at Low Tolerances. 2025 IEEE High Performance Extreme Computing Conference (HPEC), Wakefield, 15-19 September 2025, 1-9. <https://doi.org/10.1109/hpec67600.2025.11196706>
- [15] Harko, T., Lobo, F. and Mak, M.K. (2014) Analytical Solutions of the Riccati Equation with Coefficients Satisfying Integral or Differential Conditions with Arbitrary Functions. *Universal Journal of Applied Mathematics*, **2**, 109-118. <https://doi.org/10.13189/ujam.2014.020206>
- [16] Chung, D. (2007) Wavelet Characterization of Sobolev Norms. <https://www.math.unm.edu/~crisp/courses/wavelets/fall07/Sobolev.pdf>
- [17] Zeghdoudi, H., Bouchahed, L. and Dri, R. (2013) A Complete Classification of Liénard Equation. *European Journal of Pure and Applied Mathematics*, **6**, 126-136.
- [18] Valdés, J.E.N. (2025) On the Lienard's Type Equation: An Icon of the Nonlinear Analysis. <https://arxiv.org/html/2501.16637v1>
- [19] Guckenheimer, J. (2004) Bifurcations of Relaxation Oscillations. In: Ilyashenko, Y. and Rousseau, C., Eds., *Normal Forms, Bifurcations and Finiteness Problems in Differential Equations*, Kluwer Academic Publishers, 295-316. [https://pi.math.cornell.edu/~gucken/PDF/montreal\\_02.pdf](https://pi.math.cornell.edu/~gucken/PDF/montreal_02.pdf)
- [20] Szmolyan, P. and Wechselberger, M. (2004) Relaxation Oscillations in  $R^3$ . *Journal of Differential Equations*, **200**, 69-104. <https://doi.org/10.1016/j.jde.2003.09.010>
- [21] Kuehn, C. (2010) Multiple Time Scale Dynamics with Two Fast Variables and One Slow Variable. [https://www.multiscale.systems/PDF\\_files/CKuehn\\_PhD\\_thesis.pdf](https://www.multiscale.systems/PDF_files/CKuehn_PhD_thesis.pdf)
- [22] Ginoux, J.M. and Letellier, C. (2014) Van der Pol and the History of Relaxation Oscillations: Toward the Emergence of a Concept. <https://arxiv.org/pdf/1408.4890>
- [23] Hayes, M., Kaper, T., Kopell, N. and Ono, K. (1997) On the Application of Geometric Singular Perturbation Theory to Some Classical Two Point Boundary Value Problems. *International Journal of Bifurcation and Chaos*, **8**, 1-39.
- [24] Wiggins, S. (2003) Introduction to Applied Nonlinear Dynamical Systems and Chaos. Springer-Verlag.
- [25] Krupa, M. and Szmolyan, P. (2001) Relaxation Oscillation and Canard Explosion. *Journal of Differential Equations*, **174**, 312-368.

- <https://doi.org/10.1006/jdeq.2000.3929>
- [26] Mishchenko, E.F. and Rozov, N.Kh. (1980) *Differential Equations with Small Parameters and Relaxation Oscillations*. Plenum Press.
- [27] Carr, J. (1981) *Applications of Centre Manifold Theory*. Springer.
- [28] Johnson, R.S. (2005) *Singular Perturbation Theory: Mathematical and Analytical Techniques with Applications to Engineering*. Springer.  
[http://lib.ysu.am/disciplines\\_bk/906f39fcc03384c2e6b49b4f9119bf77.pdf](http://lib.ysu.am/disciplines_bk/906f39fcc03384c2e6b49b4f9119bf77.pdf)
- [29] Hunter, J.K. (2004) *Asymptotic Analysis and Singular Perturbation Theory*.  
<https://www.math.ucdavis.edu/~hunter/notes/asy.pdf>
- [30] Verhulst, F. (2007) Singular Perturbation Methods for Slow-Fast Dynamics. *Nonlinear Dynamics*, **50**, 747-753. <https://doi.org/10.1007/s11071-007-9236-z>
- [31] Sabir, A. (2022) Asymptotic and Hyperasymptotic Expansions of Solutions to ODEs. [https://people.bath.ac.uk/as5057/documents/Amins\\_Masters.pdf](https://people.bath.ac.uk/as5057/documents/Amins_Masters.pdf)
- [32] Gibson, P.C. (2025) Solution of the Scalar Riccati Equation.  
<https://arxiv.org/pdf/2508.02784v1>
- [33] Evans, L.C. (2010) *Partial Differential Equations*. 2nd Edition, American Mathematical Society.
- [34] Szmolyan, P. and Wechselberger, M. (2001) Canards in  $R^3$ . *Journal of Differential Equations*, **177**, 419-453. <https://doi.org/10.1006/jdeq.2001.4001>
- [35] Guckenheimer, J. (2008) Singular Hopf Bifurcation in Systems with Two Slow Variables. *SIAM Journal on Applied Dynamical Systems*, **7**, 1355-1377.  
<https://doi.org/10.1137/080718528>
- [36] Wechselberger, M. (2020) *Geometric Singular Perturbation Theory beyond the Standard Form*. Springer.
- [37] Kuehn, C. (2014) Normal Hyperbolicity and Unbounded Critical Manifolds. *Nonlinearity*, **27**, 1351-1366. <https://doi.org/10.1088/0951-7715/27/6/1351>